Antioxidative and Anti-UV Lignin Carrier for Peptide Delivery

Pei Lin Chee[a], Sigit Sugiarto[a], Yong Yu[a], Ying Chuan Tan[a], Enyi Ye[a*], Dan Kai[a*], Xian Jun Loh[a*]

[a.] Institute of Materials Research and Engineering (IMRE), A*STAR, 2 Fusionopolis Way, #08-03 Innovis, Singapore 138634.

Email addresses: kaid@imre.a-star.edu.sg (D. Kai), yeey@imre.a-star.edu.sg (E. Ye), lohxj@imre.a-star.edu.sg (X. J. Loh)

Abstract

Here, a sustainable antioxidant carrier based on lignin was developed to deliver palmitoyl tripeptide-38. The poly(lignin/PEG/PPG urethane) was polymerized by randomly coupling lignin, PEG and PPG segment blocks using hexamethylene diisocyanate as a crosslinker. The derived poly(lignin/PEG/PPG urethane) loaded with palmitoyl tripeptide-38, referred to as LM, was designed with careful considerations of both intrinsic and extrinsic causes of skin aging and a two-way approach was taken on to effectively target the problem of skin aging. Upon exposure to the ultraviolet irradiation, LM successfully protected the cells by reducing the presence of reactive oxygen species, the damage to the antioxidant enzymes and the expression of MMP-1. Concurrently, LM also promoted the collagen production for skin repair. It was noteworthy that the collagen I content, in cells exposed to ultraviolet irradiation with LM-4 and LM-8 treatment (LM with 4 and 8 μg/mL palmitoyl tripeptide-38 respectively), exceeded that of the control. Overall, this work successfully demonstrated a sustainable carrier with good antioxidant properties that effectively assisted the uptake of palmitoyl tripeptide-38 by the cells.

Keywords: lignocellulosic biomass, encapsulation, radical oxygen species, ultraviolet irradiation, collagen

1 Introduction

Skin aging degenerates the biological functions of skins (such as loss or disorder of collagen and glycosaminoglycans) which results in wrinkles, dyspigmentation, sallow color, dry texture and loss-of-tone. The aging of skin is a complex biological process involving both intrinsic and extrinsic factors.[1] Genetically programmed intrinsic aging is influenced by proliferation, differentiation and functional activity of skin cells together with the dermal collagen level secreted by dermal fibroblasts. Extrinsic aging is mainly caused by environmental or exogenous factors, including UV radiation, smoking, alcohol consumption and air pollution, etc. Chronic sun (UV) or chemical exposure leads to the formation of various free radical compounds, such as reactive oxygen species (ROS). These free radicals are highly reactive molecules, which tend to damage cellular structures, such as DNA, proteins, and cellular membranes, in our skin. Moreover, such free radicals may also cause locally oxidative stress-related inflammation, tissue damages or even functional disorders.

Although the necessity of cosmeceutical anti-aging intervention is debatable, the anti-oxidative theory and its approach have been widely accepted by both scientific society and the public. Various antioxidants (e.g. vitamins, lipoic acid, selenium, polyphenols, idebenone) are extensively used as ingredients in dietary and skin care products. There are several types of antioxidants that have different modes of action. One type primarily acts as free radical scavengers that are able to neutralize free radicals directly. Others target the reduction of peroxide content or quench iron to decrease ROS generation and repair oxidized membranes.

Bioactive peptides have also been used as anti-aging ingredients for skin care applications. Peptides are essential in metabolism processes including regulation of cell functionalization, melanogenesis as well as antioxidative protection of collagen degradation [2]. Palmitoyl tripeptide-38 is one of the most well-known peptides being used to reduce skin aging. It can stimulate the synthesis of collagens in skin. Experiments had demonstrated that the peptide was able to decrease skin roughness, wrinkle volume and depth, and increase density and thickness of collagen and elastin fibers in dermis [3]. However, a common issue in the topical application of peptides lies in the delivery of such molecules across the stratum corneum. These peptides are still relatively poor in terms of penetration into the skin and uptake by the skin cells.

Up to present, many studies have looked into improving the uptake of the peptides by cells. For example, there are the exploration on using chemical, physical and carrier methods. However, chemical and physical approaches are generally not preferred as the usage of chemical enhancers are prone to skin damage and irritation [4]. Physical approach can be complicated to perform, the application can be limited to charged molecules and skin damage can occur as well [4]. Microneedles has received much attention as a potential technique to overcome the barrier and being minimally invasive [5] [6]. Another method is to utilize the transdermal enhanced peptide in which the selected peptides have the ability to overcome the cell membrane impermeability [4, 7].

With the increasing demand for conventional petroleum-based materials over the past several decades, rising environmental pollution and future depletion of fossil fuels have motivated researchers to look into sustainable bio-renewable polymers. Lignocellulosic biomass is regarded as the most promising alternative in light of natural abundance and renewability. Being the second most abundant natural polymer, lignin is readily available on a large scale as the byproduct of pulp and paper industry. The recent advancement in the field of lignin-based processing coupled with lignin inherent physiochemical characteristics make it to be a potential well-deserved contender for high value biopolymers. The unique properties of lignin, such as their high activity in binding sodium salts of cholic acid, antiviral and antibacterial activities, have gained great attention for biomedical applications [8]. Additionally, lignin is an effective free radical scavenger. It consists of aromatic monomers, and it can be rationalized as the polymerization of three phenylpropanoid monomers: para-coumaryl alcohol, coniferyl alcohol, and sinapyl alcohol. These functional groups on lignin could assist to terminate the oxidation propagation reaction via hydrogen donation. As such, lignin is able to stabilize the reactions induced by oxygen and its radical species, and also inhibit enzyme activities associated with the generation of superoxide anion radicals in cancer cells to obstruct their proliferation [9]. In our previous studies, we have demonstrated that lignin-based nanofibers showed good antioxidant activities and promoted the growth of different cell types [10]. Due to its antioxidant activity, lignin has become a promising sustainable material for applications in cosmetic, pharmaceutical and food processing industries.

In this study, we developed lignin-based copolymers for the delivery of palmitoyl tripeptide-38 (Figure 1). Poly(lignin/polyethylene glycol (PEG)/polypropylene glycol (PPG) urethane) was synthesized from lignin, PEG and PPG. The chemical and thermal properties of the lignin based copolymers were characterized by NMR, GPC and DSC. Poly(lignin/PEG/PPG urethane) is capable of forming micelle in aqueous solutions, and particle size and critical micelle concentration (CMC) of the solution were studied. Performance evaluation of the poly(lignin/PEG/PPG urethane) as a carrier was conducted by encapsulating palmitoyl tripeptide-38 in the micelles. Human skin fibroblasts (HSF) treated with UVA irradiation were used as the cell aging model. Cell proliferation, collagen production, reactive oxygen species (ROS) content, the activity of diminished superoxide dismutase (SOD), catalase (CAT), glutathione peroxidase (GSH-px) and lactate dehydrogenase (LDH), malondialdehyde (MDA) production, and matrix metalloproteinases 1 (MMP-1) expression were measured to assess the efficacy of delivering the anti-aging peptides.

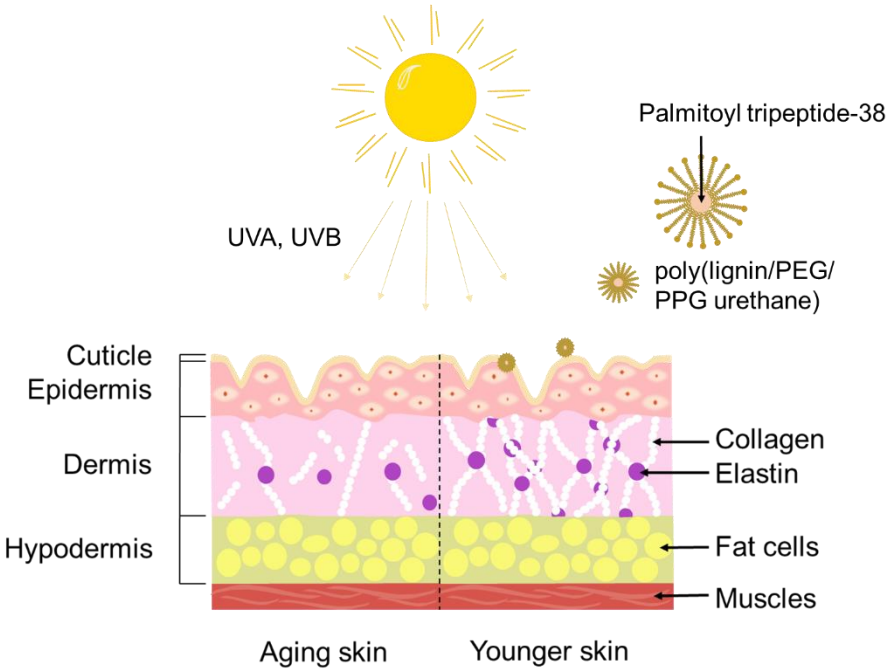

Figure 1: Illustration of poly(lignin/PEG/PPG urethane) assisting the uptake of palmitoyl tripeptide-38 by the cells leading to skin repair despite the ultraviolet radiation

2 Materials and Methods

2.1 Materials

All chemicals were purchased from Sigma-Aldrich Chemicals and used as received except where noted. Kraft lignin (average molecular weight = 5,000 g/mol) was dried at 105 °C in oven for 12 hours before use. The molecular weight of PEG and PPG were 2,000 g/mol, and 2,200 g/mol, respectively.

Dulbecco's Modified Eagle's Medium (DMEM) High Glucose, fetal bovine serum (FBS), and trypsin were purchased from Gibco Life Technologies (Carlsbad, CA, USA). Dimethyl sulfoxide (DMSO) and CCK8 kit were purchased from AMRESCO LLC (USA); ROS kit, SOD kit, MDA kit, CAT kit, GSH-px kit and LDH kit were purchased from Nanjing Jiancheng Bioengineering Institute (Nanjing, China); Human type Ⅰ collagen ELISA kit and Human type III collagen ELISA kit were purchased from RD company pack; MMP-1 antibody and β-actin antibody were purchased from abcam (Cambridge, UK). Palmitoyl tripeptide-38 was purchased from Croda.

2.2 Synthesis of poly(lignin/PEG/PPG urethane)

Poly(lignin/PEG/PPG urethane) was synthesized from the lignin, PEG and PPG with weight ratios of lignin:PEG:PPG = 5:63:32, using hexamethylene diisocyanate (HMDI) as a coupling reagent (Scheme 1). The amount of HMDI added was equivalent to the reactive hydroxyl groups in the solution. Lignin, PEG, and PPG were vacuum dried at 50 °C overnight, in a 250 ml two-neck flask. Then 0.20 g HMDI was added into the mixture and stirred for 1 hour. Next 20 ml of chloroform was added into the flask and the reaction mixture continued to stir for 24 h at 70 °C, under a nitrogen atmosphere. After reaction, diethyl ether was utilized to precipitate the resultant polymers. The final product was obtained with yield of 70%.

2.3 Characterization of poly(lignin/PEG/PPG urethane)

NMR spectrum of poly(lignin/PEG/PPG urethane) was measured at room temperature using Bruker AV-400 NMR spectrometer in $CDCl_3$ solvent. Molecular weight (M_n and M_w) and polydispersity index of polymer were analyzed by Waters gel permeation chromatography (GPC, a Shimadzu SCL-10A and LC-8A system equipped with two Phenogel 5 mm 50 and 1000 Å columns in series and a Shimadzu RID-10A refractive index detector) using HPLC grade tetrahydrofuran as an eluent. The flow rate of tetrahydrofuran eluent was 1.0 ml/min at

25 °C. The average molecular weights were determined with a calibration based on linear poly(methyl methacrylate) standards.

Thermal behavior of the polymer was also investigated and performed on Thermogravimetric analysis (TGA, Q500, TA Instruments, USA) and differential scanning calorimeter (DSC, Q100, TA Instruments, USA). For TGA, the sample was heated at 20 °C/min from room temperature to 600 °C in a dynamic nitrogen atmosphere (flow rate = 60 ml/min). DSC is equipped with an auto cool accessory and calibrated using indium. The following protocol was used for test: heating from -50 °C to +100 °C at 20 °C/min, holding at +100 °C for 5 min, cooling from +100 °C to -50 °C at 20 °C/min, and finally reheating from -50 °C to +100 °C at 20 °C/min. Melting temperature (T_m) and melting enthalpy change (ΔH_m) was determined from the endothermic melting peak from the second heating run.

Particle size of poly(lignin/PEG/PPG urethane) in water and its critical micelle concentration (CMC) were determined using a Malvern Zetasizer, NANO ZS (Malvern Instruments Limited, U.K.) equipped with a 4 mW He–Ne laser operating at a wavelength of 633 nm. Measurements were carried out in a polystyrene cell at 25 °C. A series of poly(lignin/PEG/PPG urethane) solutions ranging from 0.5 wt% to 0.0001 wt% were prepared from an aqueous stock solution of 1 wt%. Data processing was carried out with a computer attached to the instrument. The CMC value was determined by plotting a graph of the count rate versus the logarithmic copolymer concentration. The stability of 0.5 wt% poly(lignin/PEG/PPG urethane) in phosphate-buffered saline (PBS) and medium was measured on day 0, 1, 3, 5, 7, 10 and 14. The morphology of poly(lignin/PEG/PPG urethane) micelle was characterized by transmission electron microscopy (TEM).

The antioxidant activity of the poly(lignin/PEG/PPG urethane) was evaluated by 1,1-diphenyl-2-picrylhydrazyl (DPPH) assay [11]. 10 mg of the copolymer were placed in 15 ml glass vials. A 60 μM DPPH solution was prepared in methanol, and 10 ml of such solution was added into each vial. DPPH free radical content was measured by monitoring the absorbance changes at 517 nm at each time point. All samples were prepared in triplicate. The antiradical activity was measured as % inhibition of free radicals by measuring the decrease in absorbance compared to control solutions. Pluronic F127 was used as control.

2.4 Cell culture

Human skin fibroblasts cell line (HSF) was purchased from the Chinese Academy of Sciences Shanghai cell bank (Shanghai,China). Cells were maintained in DMEM supplemented with 10% FBS, 1% penicillin and 1% streptomycin in a cell incubator with 5% CO_2 at 37 °C.

2.5 Cytotoxicity evaluation

Cytotoxicity of the poly(lignin/PEG/PPG urethane) was evaluated with cell titer blue assay on NIH/3T3 cells. 5000 cells were seeded and incubated at 37°C under 5% carbon dioxide and 95% relative humidity atmosphere for 24 h. Poly(lignin/PEG/PPG urethane) was introduced to the wells and allowed to incubate for 24h, 48h or 72h. Subsequently, cell titer blue assay was added and incubated for another 3h before measurements were taken at excitation and emission wavelength of 560nm and 590nm respectively.

2.6 UVA irradiation

HSF cells were seeded on culture dishes washed with phosphate-buffered saline (PBS) once after incubation and then exposed to UVA (10 J/cm^2). UVA irradiated doses were calculated by ultraviolet intensity measurement (UV340B, China Sampo Ltd. Shenzhen, China). After exposure to UVA, cells were incubated in DMEM for 24 h. In parallel, control cells were treated under the same conditions without UVA irradiation.

2.7 Intracellular ROS measurement

Intracellular ROS level was evaluated by 2,7-dichlorfluorescein diacetate (DCFH-DA) assay. HSF cells were seeded in 96-well culture plates (80% filled) at a density of 5×10^4 cells/well and incubated at 37 ℃. After irradiation with10 J/cm^2 UVA, the cells were incubated with different concentrations of palmitoyl tripeptide-38 for 24 h. Subsequently, cells were further incubated with 50 μL 10 μmol L^{-1} DCFH-DA for 20 min and washed three times with serum-free DMEM. The fluorescence intensity was detected at 488 nm excitation and 525 nm emission and quantified using a fluorescence microplate reader (Synergy HT, BioTek, USA).

2.8 Measurement of MDA content

Oxygen radicals elicit membrane peroxidation and MDA formation, which are detrimental to cellular function. MDA production was evaluated in cell lysates using the MDA regent kit according to the manufacturer's instructions.

2.9 Determination of the activities of SOD, CAT and GSH-Px

HSF cells were seeded in 96-well plates at the density of 1×10^5 cells/well with or without treatment with palmitoyl tripeptide-38 for 24 h followed by UVA irradiation. The activities of SOD, CAT and GSH-Px were determined using relevant commercial kits in accordance with the instruction manual.

2.10 Cell viability assay

Cellular viability was assessed with cell counting kit-8 and lactate dehydrogenase (LDH) release assays. HSF cells were trypsinized, seeded at 5×10^4 cells/wellin 96-well plates, exposed to UVA irradiation and incubated for 72 h. The cells were then treated with different concentrations of palmitoyl tripeptide-38. Subsequently, 20 μl of CCK-8 solution was added into each well and 100 μl of serum-free medium was added into the control cells. After incubation for 1 h at 37 ℃, absorbance at 450 nm for each well was measured using a microplate reader (Synergy HT, BioTek, Winooski, VT, USA). LDH release was monitored with the Cytotoxicity Detection Kit LDH in cell-free culture supernatants.

2.11 Western blotting analysis

Cells were seeded in 96-well plates at the density of 1×10^5 cells/well with or without treatment with palmitoyl tripeptide-38 for 24 h after UVA irradiation. The treated cells were washed twice with cold PBS and homogenized in 1ml RIPA protein lyaste at 12 000 rpm for 15 min at 4 ℃. Protein concentration was measured by a BCA protein assay kit. Aliquot of the supernatant, containing equal amounts of proteins, were electrophoresed on 10% separation gel and 5% concentrated gel and then transferred onto nitrocellulose membranes (Amersham Pharmacia Biotech., England, UK). The membranes were washed twice with Tris/buffered saline (TBS) and blocked in the 5% skimmed milk powder of confining liquid for 1h at 37℃.

Subsequently, they were transferred into TBST and incubated for 2 h at room temperature with appropriate concentrations of primary antibodies (β-actin was 1: 3000 dilution, MMP-1 was 1: 1000 dilution). The probed membranes were washed with TBST three times, 10 min for each, and then incubated with secondary antibodies for 2 h in the same way. Western blot was repeated three times under the same conditions independently for the assessment of intra-experimental variability. Immunobands were detected on ECL reagents and quantified using Tanon T600 image analysis system (Shanghai Tanon Technology Ltd. Shanghai, China). β-actin was considered as a loading control.

2.12 Collagen content measurement

Cells were seeded in 96-well plates at the density of 1×10^5 cells/well with or without treatment with palmitoyl tripeptide-38 for 24 h after UVA irradiation. The content of human type I collagen and type III collagen were determined using relevant commercial kits in accordance with the instruction manual.

2.13 Statistical analysis

Each experiment was repeated at least 3 times. All data were expressed as mean ± standard deviation ($\bar{x} \pm s$). The significance test was analyzed by SPSS19.0 software. Differences between groups were analyzed by variance analysis, $P<0.05$ or $P<0.01$ was considered as a significant.

3 Results and discussion

3.1 Synthesis and characterization of poly(lignin/PEG/PPG urethane)

Kraft lignin is difficult to dissolve in water (pH 7) and many organic solvents, which limits its surface modification and applications. In this study, we reported a simple method to synthesize water soluble lignin-based polyurethane. Poly(lignin/PEG/PPG urethane) was polymerized by randomly coupling lignin, PEG and PPG segment blocks using HMDI with dibutyltin dilaurate as the catalyst. The synthesis route of the poly(lignin/PEG/PPG urethane) is shown in Scheme 1. The chemical structure of poly(lignin/PEG/PPG urethane) prepared in $CDCl_3$ was verified

by ^{1}H NMR (Figure S1). All proton signals belonging to PEG and PPG segments were observed (δ 4.92-4.87 (m, C*H* of PPG unit), 4.46-4.44 (m, CH_2 of PPG unit), 4.21-4.19 (t, CH_2 of PEG unit), 3.79-3.76 (t, CH_2 of PPG unit), 3.66-3.64 (m, C*H* and CH_2 of PPG unit, CH_2 of PEG unit), 3.58-3.39 (m, CH_2 of PPG unit), 1.14-1.12 (CH_3 of PPG unit)). The signals of HMDI were identified at 3.16-3.13 ppm (NHCH_2), 1.50-1.47 ppm (NHCH$_2$CH_2), 1.33-1.30 ppm (NHCH$_2$CH$_2$CH$_2$). The signal of lignin methoxyl groups (3.7 ppm) was overlapped with the peaks of PPG and PEG. The molecular weight of poly(lignin/PEG/PPG urethane) was 9.8 kDa for Mn and 11.7 kDa for Mw, determined by GPC. The obtained poly(lignin/PEG/PPG urethane) was soluble in water and many commonly used organic solvents (e.g. chloroform, THF, acetone), forming uniform light yellow solutions (Figure S2).

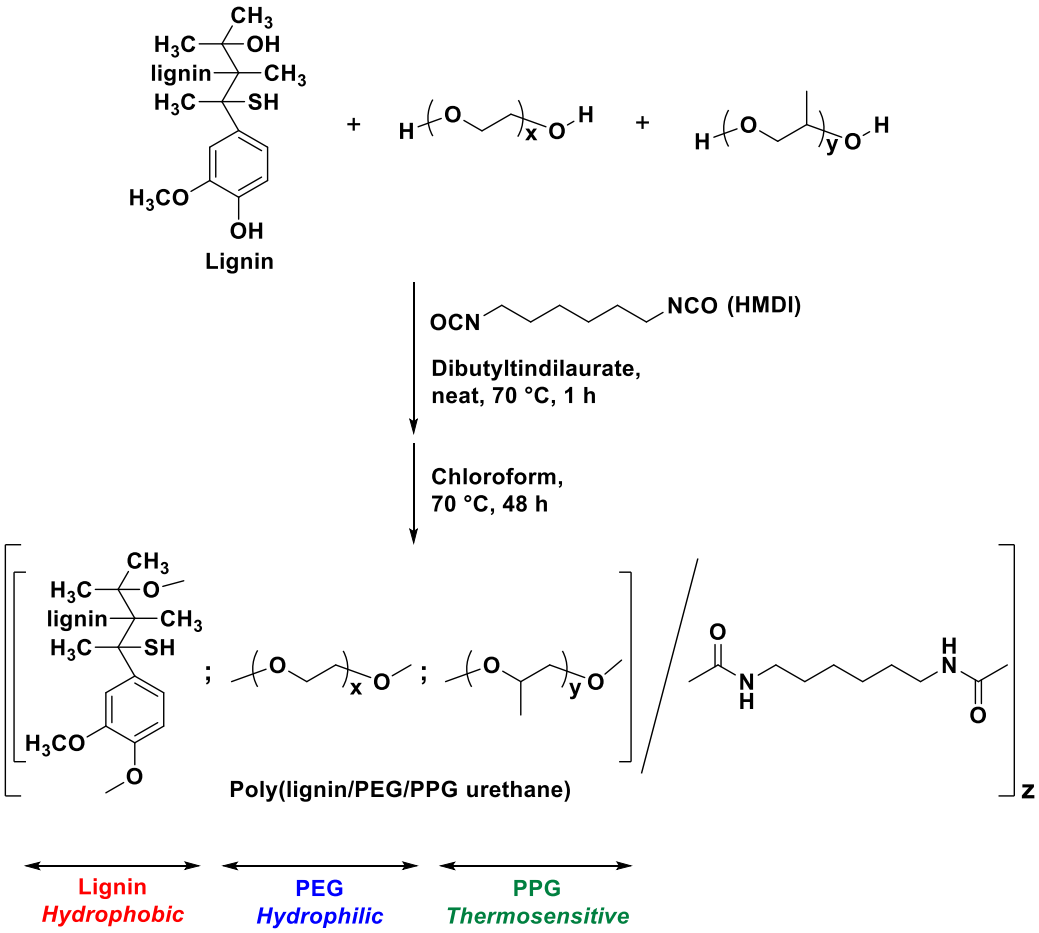

Scheme 1 Illustration of the synthesis reaction

The thermal properties of poly(lignin/PEG/PPG urethane) were characterized by TGA and DSC. Under N_2 atmosphere, kraft lignin thermally decomposed very slowly. Its decomposition temperature (T_d, @ 5% weight loss) was 260 °C and large amount of carbon residual (almost 60%) remained even at 500 °C (Figure S3). Unlike raw lignin, poly(lignin/PEG/PPG urethane) showed similar decomposition profile as PEG-PPG copolymers (Figure S4A). T_d and

derivative peak temperatures of poly(lignin/PEG/PPG urethane) were found at 337 °C and 417 °C respectively. The amount of carbon residual at 500 °C was only 3.2%. DSC result shows that the poly(lignin/PEG/PPG urethane) was a semi-crystalline polymer with a melting temperature (T_m) of 44 °C and an enthalpy of 124 J/g (Figure 5B). The thermal behaviour was similar to the commonly used PEG-PPG copolymers, pluronic F127, which has a T_m of 49 °C and an enthalpy of 112 J/g (Figure S5).

3.2 UV absorption capability of poly(lignin/PEG/PPG urethane)

The results of the UV spectroscopy shows that poly(lignin/PEG/PPG urethane) (Figure 2A) had broad absorbance across UV-A to UV-C ranges. It strongly absorbed within the more harmful UV-C range (200 to 280 nm) and UV-B ranges (280 to 315 nm). It also absorbed in the UV-A (315 to 400 nm). A characteristic absorption maxima was visible at around 280 nm which could be attributed to the abundance of aromatic phenolic groups present in the structure of lignin. This demonstrated good UV performance of the material.

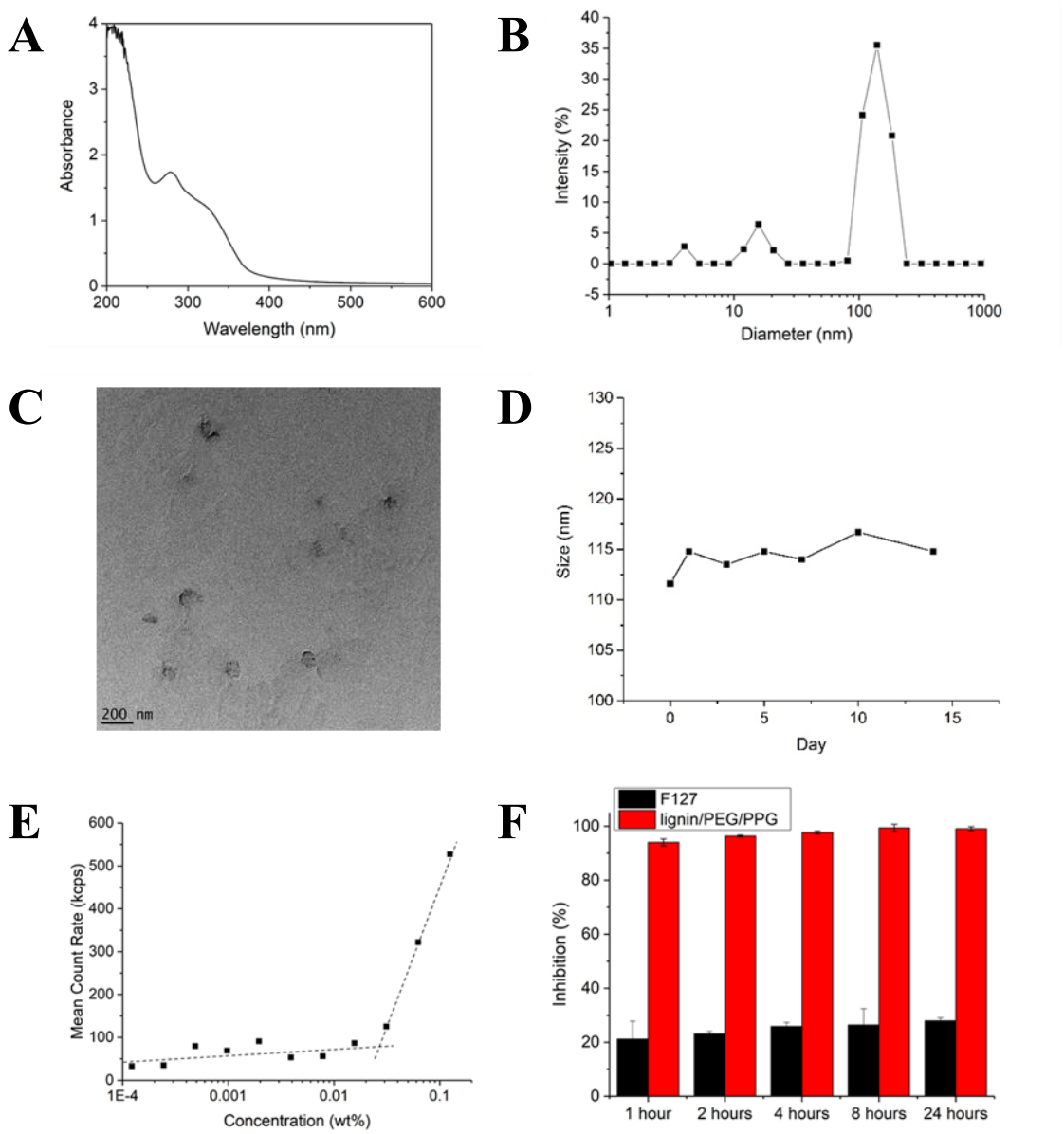

Figure 2 Graph displaying the absorbance of poly(lignin/PEG/PPG urethane) against different wavelengths (A); Size distribution of 0.5 wt% poly(lignin/PEG/PPG urethane) aqueous solution obtained by DLS (B); TEM image of 1 wt% poly(lignin/PEG/PPG urethane) (C); Stability of poly(lignin/PEG/PPG urethane) in PBS measured across 14 days (D); Mean count rates (kcps) as a function of poly(lignin/PEG/PPG urethane) concentration (E); Free radical inhibition (an indication of the antioxidant activity) of poly(lignin/PEG/PPG urethane) and F127 (control) measured by DPPH assay (F)

3.3 Micelle properties of poly(lignin/PEG/PPG urethane)

The micelle properties of the water-soluble poly(lignin/PEG/PPG urethane) were studied with the use of DLS. DLS is a commonly used technique to detect particle size in colloidal dispersions. Poly(lignin/PEG/PPG urethane) was dissolved in DI water to form 0.5 wt% aqueous solution, and DLS results shows that the average particle size of the copolymer was 96.6 nm with a PDI of 0.46 (Figure 2B), indicating that the poly(lignin/PEG/PPG urethane) was able to form micelles in water. The TEM image (Figure 2C) shows that most of the round micelles exhibited uniform size (~100 nm), which is consistent to the DLS result. Additionally, it was found that micelles formed from poly(lignin/PEG/PPG urethane) was relatively stable for the tested period (Figure 2D and S6). The micelles formed in PBS displayed size that ranged between 111nm and 117nm. Hence, the critical micelle concentration (CMC) determination was carried out for the poly(lignin/PEG/PPG urethane) at 25 °C. Besides particle size, DLS is also suitable for studying micellization phenomena and determination of the CMC values. This experiment was conducted by varying the aqueous polymer concentration in the range of 0.0001 to 0.5 wt%. The mean count rates (representing the average scattering intensity) as a function of poly(lignin/PEG/PPG urethane) concentration are shown in Figure 2E. For concentration higher than the CMC, the mean count rates reduced linearly with decreasing poly(lignin/PEG/PPG urethane) concentration. This implies that the dilution decreased the number of micelles in the solution. At concentration below CMC, the mean count rates showed an approximately constant value regardless of the change in concentration, suggesting no micelle formation in this range of concentration. The CMC value of the poly(lignin/PEG/PPG urethane) was obtained as ~ 0.027 wt%, determined by the intersection of the best fit lines drawn through the data point.

3.4 Antioxidant properties of poly(lignin/PEG/PPG urethane)

The antioxidant activities of poly(lignin/PEG/PPG urethane) were evaluated by DPPH assay. As shown in Figure 2F, F127 had very low antioxidant activities with 27.9 ± 1.1 % free radical inhibition even after 24 hours, while poly(lignin/PEG/PPG urethane) exhibited good antioxidant properties. After one hour incubation, poly(lignin/PEG/PPG urethane) already displayed very high free radical inhibition of 94.0 ± 1.3%. Lignin is a natural antioxidant agent and it contains a high content of phenolic moieties which can prevent the proliferation of free radicals. Every day, our skin is exposed to damage from all kinds of free radical compounds. The presence of these free radicals in the skin could cause skin damage, ranging from aging, pigment darkening to skin cancer [12]. The application of poly(lignin/PEG/PPG urethane) could

terminate the propagation of free radicals and potentially reduce localized oxidative stress in our skin.

3.5 Cytotoxicity Evaluation

With the intention to use poly(lignin/PEG/PPG urethane) as a potential cosmetic, its biocompatibility was investigated. Two concentrations were tested and it was incubated up to 72 hours with the cells. With reference to Figure 3, the results show that the developed poly(lignin/PEG/PPG urethane) was highly compatible with the cells with more than 80% cell viability detected even after 72 hours incubation.

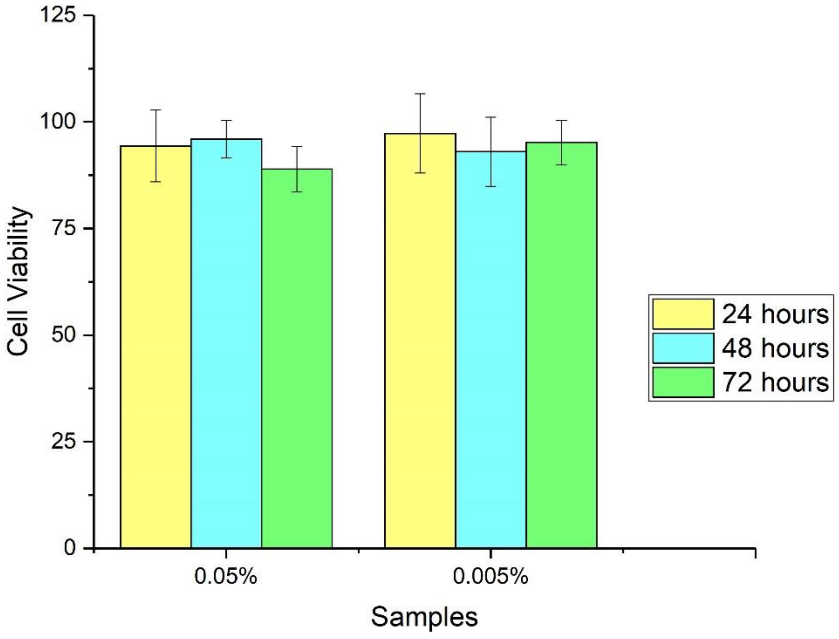

Figure 3 Cell viability of 3T3 cells after 24h, 48h and 72h incubation with poly(lignin/PEG/PPG urethane)

3.6 ROS generation and MDA content in UVA-induced HSF cells

While reactive oxygen species (ROS) are essential intermediates in oxidative metabolism, excess ROS could induce undesirable oxidative stresses that damage cells by peroxidizing lipids and disrupting structural proteins, enzymes and nucleic acids. With the aim to use poly(lignin/PEG/PPG urethane) as the carrier for palmitoyl tripeptide-38 and also to provide antioxidant activity, it would be relevant to examine if the encapsulation of the peptide would

affect the capability of the poly(lignin/PEG/PPG urethane) in serving its latter function. Hence, different concentrations of the peptides were encapsulated in the the poly(lignin/PEG/PPG urethane) micelles and the system would be subsequently referred to as LM. An indication of the antioxidant activity could be deduced from the amount of intercellular ROS generation, which was examined through the use of DCFH-DA fluorescence intensity measurement. As shown in Figure 4A, ROS generated by HSF cells exposed to UVA-alone (model group) attained 416 MFI, which was a 2.07-fold increment as compared to the control cells (not subjected to UVA irradiation and LM treatment). The treatment with 2, 4 and 8 μg/mL of LM were shown capable of inhibiting UVA-induced ROS generation to 396.88±12.55, 305.05±19.57 and 264.50 ± 17.91, respectively.

Lipid peroxidation is a well-known process to indicate the oxidative stress in cells and tissues [13]. Free radicals degrade polyunsaturated fatty acids and generate malondialdehyde (MDA) [14]. Therefore, MDA is a widely used biomarker for lipid peroxidation and oxidative stress. As shown in Figure 4B, HSF cells exposed to UVA alone (model group) showed significant increase in MDA content from 0.56 ± 0.05 nmol/mgprot (control) to 0.82 ± 0.06 nmol/mgprot. The introduction of LM to the UVA-induced HSF cells showed a dose-dependent decrease in the MDA content and there was a statistically significant difference versus model group.

Hence, these results suggest that the poly(lignin/PEG/PPG urethane) is a suitable carrier for the palmitoyl tripeptide-38. The encapsulation of the peptides did not adversely affect its antioxidant properties.

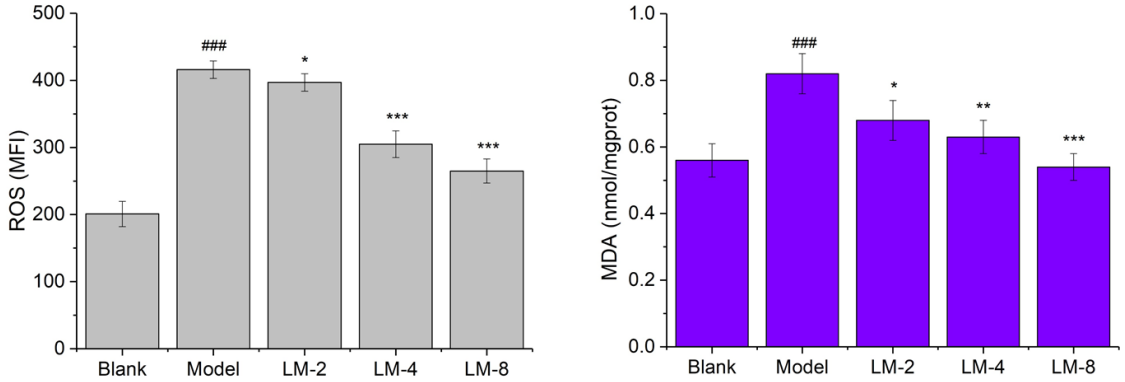

Figure 4 Effect of LM on ROS generation (A) and MDA content (B) in UVA-induced HSF cells ###P<0.001 vs. the blank control; *P<0.05, ** P<0.01 and *** P<0.001 vs. the model group (UVA-alone)

3.7 Activities of SOD, CAT and GSH-Px in UVA-induced HSF cells

Three main antioxidant enzymes (Superoxide dismutase (SOD), catalase (CAT), and glutathione peroxidase (GSH-Px)) in cells were selected to provide further insights into the antioxidant activities of LM on HSF cells. These enzymes work together to defend against oxygen-derived free radicals. SOD catalyses the conversion of superoxide anion into hydrogen peroxide (H_2O_2), whereas CAT and GSH-Px reduce H_2O_2 into H_2O and O_2 [15]. Previous studies have shown that SOD family could protect cells from UV radiation and the consequential skin damage [16, 17]. CAT could reduce the damage to DNA caused by UV radiation [16, 18]. Hence, antioxidant enzyme activities of SOD, CAT and GSH-Px were examined using relative kits to evaluate the protective effect of LM on the antioxidant-defense system. Compared with the control, SOD, CAT and GSH-Px activities of HSF cells exposed to UVA alone (model group) significantly decreased to 3.82 ± 0.35 NU/mgprot, 25.08 ± 3.57 U/mgprot and 55.17±2.80 U/mgprot respectively. The results were not surprising as it had been demonstrated that the ultraviolet radiation could cause apoptosis and NETosis [19]. In contrary, UVA-induced HSF cells treated with LM showed dose-dependent increase in SOD, CAT and GSH-Px activities and statistically significant differences versus model group (Figure 5). In fact, LM-4 and LM-8 appeared to have almost maintained the same level of SOD activity and CAT activity in the cells as the control, that was not exposed to UVA irradiation. Thus, LM treatment was considered to be effective in protecting the cells and its antioxidant defense system against UV irradiation.

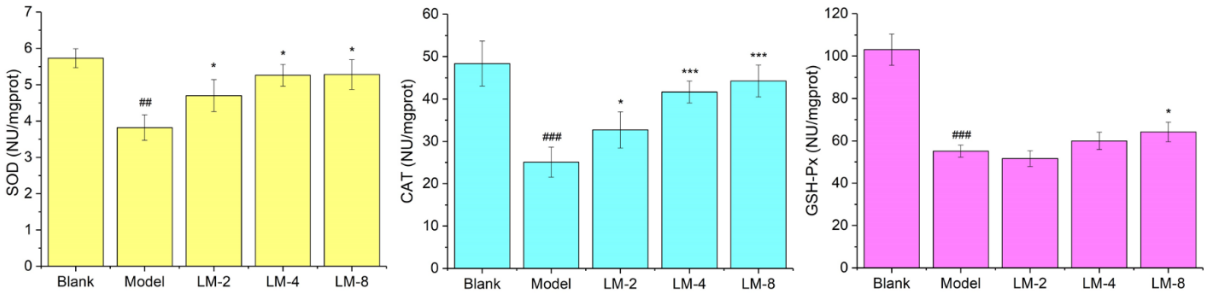

Figure 5 Effect of LM on SOD activity (A), CAT activity (B) and GSH-Px activity (C) in UVA-induced HSF cells $^{###}P<0.001$ and $^{##}P<0.01$ vs. the blank control; $^{*}P<0.05$ and $^{***}P<0.001$ vs. the model group (UVA-alone)

3.8 Effect of LM on UVA-induced cytotoxicity in HSF cells

In order to further substantiate the UV shielding of LM and the explanation for the drop in the level of antioxidant enzyme activities, CCK-8 assay and LDH activity measurements were performed. As shown in Table 1, UVA exposure significantly reduced HSF cell viability to 50.59% as compared with the control cells. In contrast, the viability of HSF cells increased along with the applied LM concentration achieving 55.87%, 65.40% and 71.98% with the use of LM containing 2, 4 and 8 μg/mL of palmitoyl tripeptide-38 respectively. Correspondingly, LDH activity in UVA-induced HSF cells decreased significantly with increasing concentration of LM (Table 1). LDH is an important marker associated with tissue damage in our body as it is only released substantially during injuries and diseases. Our results demonstrate that LM had the capability to protect HSF cells from UV irradiation.

Table 1. Effect of LM on UVA-induced cytotoxicity in HSF cells

Samples	**Absorbance value(OD 450nm)**	**Survival rate**	**LDH (U/L)**
Blank	1.84 ± 0.02	100%	533 ± 57
Model group	$0.93 \pm 0.03^{\#\#\#}$	50.59%	$1629 \pm 97^{\#\#\#}$
LM-2	$1.03 \pm 0.05^{*}$	55.87%	$1323 \pm 139^{**}$
LM-4	$1.20 \pm 0.01^{***}$	65.40%	$827 \pm 67^{***}$
LM-8	$1.32 \pm 0.03^{***}$	71.98%	$703 \pm 43^{***}$

$^{\#\#\#}P<0.001$ vs. the blank control; $^{*}P<0.05$ and $^{***}P<0.001$ vs. the model group (UVA-alone).

3.9 Expression of MMP-1 in UVA-induced HSF cells

Besides inducing the ROS generation, the exposure to sunlight also elevates the matrix metalloproteinase-1 (MMP-1) content [20], which is the enzyme responsible for collagen digestion. Collagen is one of the main structural substance in our body and also, our skin. Collagen fibers established the matrix of our skin providing integrity, firmness and elasticity to the structure. Therefore, a high level of MMP-1 is usually associated with photoaging. In order to achieve maximum anti-aging effect, it would be advantageous for the treatment to

target both ROS generation as well as the expression of MMP-1. In our investigation, it appears that the increased encapsulation of palmitoyl tripeptide-38 led to decline in MMP-1 expression (Figure 6A and Figure 6B). These results suggest good efficacy of LM in reducing MMP-1 expression, which could possibly translate to lesser collagen digestion.

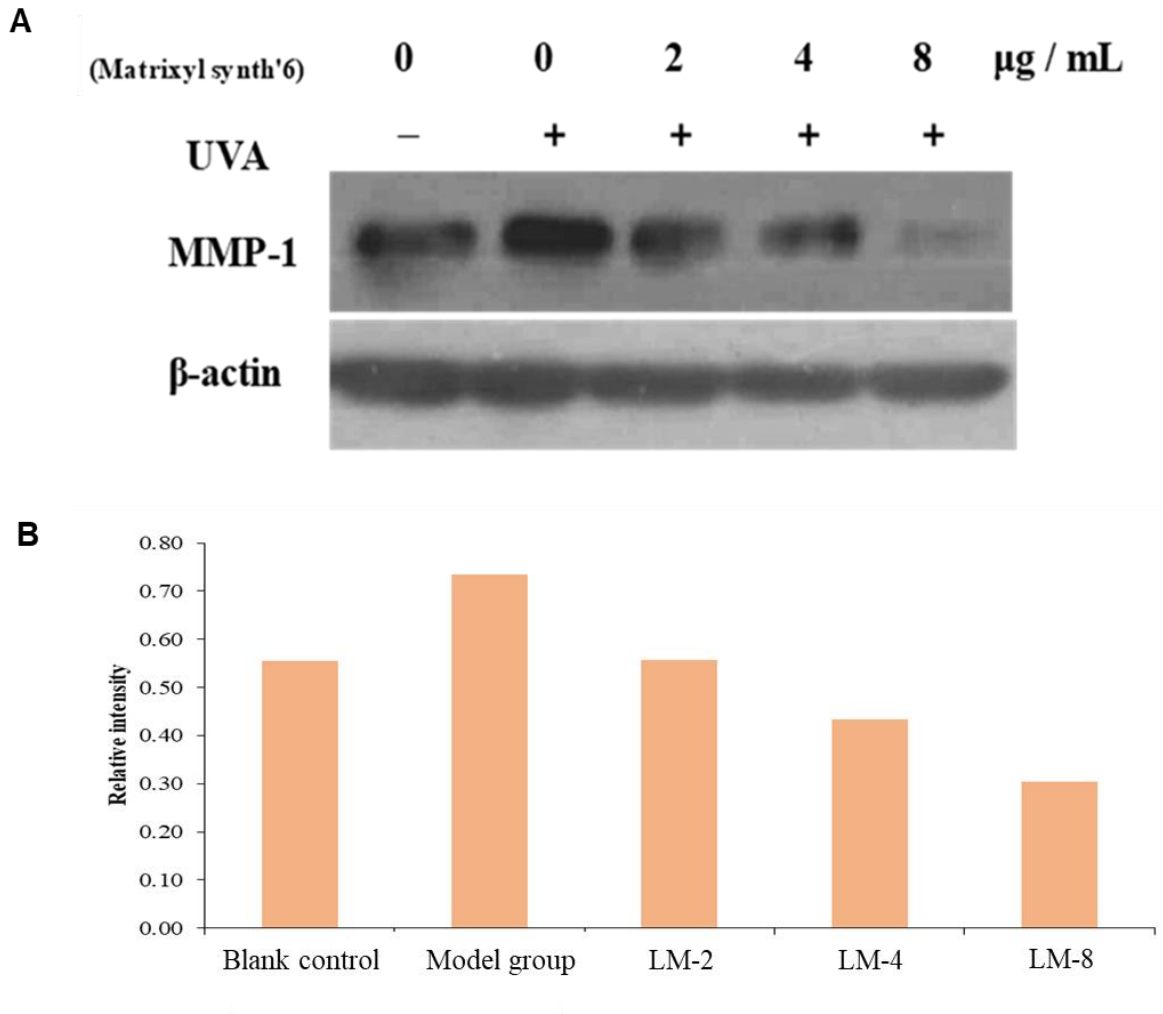

Figure 6 Expression of MMP-1 in UVA-induced HSF cells (A) and its relative intensity of expression after treated with different dosages of palmitoyl tripeptide-38 (B)

3.10 Collagen content in UVA-induced HSF cells

Next, study was performed to assess if the effect of palmitoyl tripeptide-38 was successfully delivered via LM. There are many types of collagen in our body, each serving a different function to support the normal functioning of the body. The collagen present in the skin are predominantly collagen type I and III. In this study, ELISA assay was conducted to examine

the ability of LM to maintain the collagen contents in the HSF cells after subjected to UVA irradiation. As shown in Figure 7, UVA exposure of HSF cells significantly reduced type I collagen content to 22.86 ± 2.07 ng/mL as compared with the control cells. The groups that were treated with 2, 4 and 8 μg/mL of LM were observed with higher type I collagen content in UVA-induced HSF cells, which was attained up to 31.81 ± 2.05, 63.37 ± 6.48 and 72.06 ± 3.5 ng/mL respectively. Similarly, UVA exposure significantly reduced type III collagen content in HSF cells from 19.32 ±1.7 ng/mL to 7.28 ± 0.94 ng/mL (Figure 7). In contrast, the type III collagen content in UVA-induced HSF cells treated with LM at concentrations of 2, 4 and 8 μg/mL increased significantly to 10.65 ± 0.67, 16.24 ± 1.49 and 22.15 ± 2.01ng/mL respectively.

It was noteworthy that the collagen I content obtained after LM-4 and LM-8 treatment exceeded the control group. The intended function of palmitoyl tripeptide-38 displayed through the elevated collagen I content signifies that poly(lignin/PEG/PPG urethane) is a suitable peptide carrier. Additionally, palmitoyl tripeptide-38 has been demonstrated previously as a powerful peptide to promote the production of collagen type I in *in vitro* cell culture studies. Hamley et al. reported that 80 μg/mL of palmitoyl tripeptide-38 doubled the collagen content produced from human corneal and dermal fibroblasts as compared with the basal media [3]. Compared to their findings, our LM with 10-time lower concentration (8 μg/mL) was able to increase 3 times of collagen production even after UV treatment. This result indicated that the LM capsules could not only protect skin cells from UV damage, but also stimulate the cells to release more collagen for skin repair.

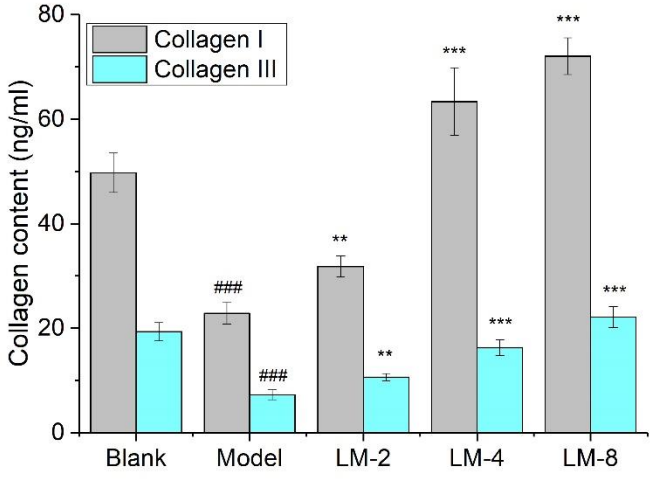

Figure 7 Effect of LM on type I and type III collagen content in UVA-induced HSF cells $^{###}P<0.001$ vs. the blank control; $^{**}P<0.01$ and $^{***}P<0.001$ vs. the model group (UVA-alone)

4 Conclusion

In this work, a lignin-based carrier was developed to deliver palmitoyl tripeptide-38 into the cells overcoming the penetrating difficulty of large peptide. The two-way approach utilized in this study placed the emphasis on simultaneously minimizing damages and promoting repair. It seems promising with the decreased ROS generation, MDA content and MMP-1 expression. UVA-induced HSF cells treated with LM showed dose-dependent increase in SOD, CAT and GSH-Px activities. Higher cell viability and reduced LDH activity were associated with higher concentration of LM used. Additionally, the established system promoted the collagen production for skin repair. It was noteworthy that the collagen I content obtained after LM-4 and LM-8 treatment exceeded that of the control. Hence, this work successfully demonstrated a possible way to valorize lignin to sustainable peptide carrier, that exhibited good antioxidant properties without adverse effect on the peptide.

CRediT authorship contribution statement

Pei Lin Chee: Investigation, Methodology, Visualization, Writing – original draft, Formal analysis. Sigit Sugiarto, Yu Yong & Tan Ying Chuan: Investigation, Methodology, Writing – original draft. Enyi Ye: Investigation, Methodology, Conceptualization. Dan Kai: Supervision, Methodology, Writing – review & editing, Conceptualization, Validation. Xian Jun Loh: Conceptualization

Conflicts of interest

There are no conflicts to declare.

Acknowledgements

The authors gratefully acknowledge the financial support from Agency for Science, Technology and Research (A*STAR).

5 References

[1] M. Liu, J. Tao, H. Guo, L. Tang, G. Zhang, C. Tang, H. Zhou, Y. Wu, H. Ruan, X. J. Loh, Materials 2021, 14, 4458; X. J. Loh, D. J. Young, H. Guo, L. Tang, Y. Wu, G. Zhang, C. Tang, H. Ruan, Materials 2021, 14, 2797.

[2] N. Lourith, M. Kanlayavattanakul, J. Cosmet. Laser Ther. 2016, 18, 301.

[3] R. R. Jones, V. Castelletto, C. J. Connon, I. W. Hamley, Mol. Pharm. 2013, 10, 1063.

[4] R. Ruan, M. Chen, L. Zou, P. Wei, J. Liu, W. Ding, L. Wen, Therapeutic Delivery 2016, 7, 89.

[5] M. Avcil, G. Akman, J. Klokkers, D. Jeong, A. Çelik, Journal of Cosmetic Dermatology 2020, 19, 328.

[6] Y. H. Mohammed, M. Yamada, L. L. Lin, J. E. Grice, M. S. Roberts, A. P. Raphael, H. A. Benson, T. W. Prow, PloS one 2014, 9, e101956.

[7] L. B. Lopes, C. M. Brophy, E. Furnish, C. R. Flynn, O. Sparks, P. Komalavilas, L. Joshi, A. Panitch, M. V. L. B. Bentley, Pharmaceutical Research 2005, 22, 750.

[8] V. Ugartondo, M. Mitjans, M. P. Vinardell, Bioresour. Technol. 2008, 99, 6683.

[9] T. Dizhbite, G. Telysheva, V. Jurkjane, U. Viesturs, Bioresour. Technol. 2004, 95, 309; F. J. Lu, L. H. Chu, R. J. Gau, Nutr Cancer 1998, 30, 31.

[10] D. Kai, W. Ren, L. Tian, P. L. Chee, Y. Liu, S. Ramakrishna, X. J. Loh, ACS Sustain. Chem. Eng. 2016.

[11]R. van Lith, E. K. Gregory, J. Yang, M. R. Kibbe, G. A. Ameer, Biomaterials 2014, 35, 8113; N. Baheiraei, H. Yeganeh, J. Ai, R. Gharibi, M. Azami, F. Faghihi, Mater. Sci. Eng. C-Mater. Biol. Appl. 2014, 44, 24.

[12] L. Borska, C. Andrys, J. Krejsek, V. Palicka, V. Vorisek, K. Hamakova, J. Kremlacek, P. Borsky, Z. Fiala, J Dermatol Sci 2016, 81, 192; A. K. Srivastav, S. F. Mujtaba, A. Dwivedi, S. K. Amar, S. Goyal, A. Verma, H. N. Kushwaha, R. K. Chaturvedi, R. S. Ray, J. Photochem. Photobiol. B-Biol. 2016, 156, 87.

[13] S. Gaweł, M. Wardas, E. Niedworok, P. Wardas, Wiadomosci lekarskie (Warsaw, Poland : 1960) 2004, 57, 453.

[14] D. R. Janero, Free Radic. Biol. Med. 1990, 9, 515; A. Khalil, K. Maryam, J. Abolghasem, BioImpacts 2015, 5, 123.

[15] X. Ma, D. Deng, W. Chen, in *Enzyme Inhibitors and Activators*, (Ed: M. Senturk), InTech, Rijeka 2017, Ch. 09.

[16] A. M. Pudlarz, E. Czechowska, M. S Karbownik, K. Ranoszek-Soliwoda, E. Tomaszewska, G. Celichowski, J. Grobelny, E. Chabielska, A. Gromotowicz-Popławska, J. Szemraj, Nanomedicine 2020, 15, 23.
[17] G. Palmieri, S. Arciello, M. Bimonte, A. Carola, A. Tito, M. Gogliettino, E. Cocca, C. Fusco, M. Balestrieri, M. G. Colucci, F. Apone, Journal of Biotechnology 2019, 302, 101.
[18] V. Lee, M. D. Gober, H. Bashir, C. O'Day, I. A. Blair, C. Mesaros, L. Weng, A. Huang, A. Chen, R. Tang, V. Anagnos, J. Li, S. Roling, E. Sagaityte, A. Wang, C. Lin, C. Yeh, C. Atillasoy, C. Marshall, T. Dentchev, T. Ridky, J. T. Seykora, Experimental Dermatology 2020, 29, 29.
[19] D. Azzouz, M. A. Khan, N. Sweezey, N. Palaniyar, Cell Death Discovery 2018, 4, 51.
[20] R. I. Amer, S. M. Ezzat, N. M. Aborehab, M. F. Ragab, D. Mohamed, A. Hashad, D. Attia, M. M. Salama, M. H. El Bishbishy, Biomedicine & Pharmacotherapy 2021, 138, 111537.